Vol. 511: 41–58, 2014
doi: 10.3354/meps10933

MARINE ECOLOGY PROGRESS SERIES
Mar Ecol Prog Ser

Published September 24

Spatio-temporal variability in ammonia oxidation and ammonia-oxidising bacteria and archaea in coastal sediments of the western English Channel

K. Tait[1,*], V. Kitidis[1], B. B. Ward[2], D. G. Cummings[1], M. R. Jones[1], P. J. Somerfield[1], S. Widdicombe[1]

[1]Plymouth Marine Laboratory, Prospect Place, Plymouth, PL1 3DH, UK
[2]Department of Geosciences, Guyot Hall, Princeton University, Princeton, NJ 08544, USA

ABSTRACT: The abundance of ammonia-oxidising bacterial (AOB) and ammonia-oxidising archaeal (AOA) (*amoA*) genes and ammonia oxidation rates were compared bimonthly from July 2008 to May 2011 in 4 contrasting coastal sediments in the western English Channel. Despite a higher abundance of AOA *amoA* genes within all sediments and at all time-points, rates of ammonia oxidation correlated with AOB and not AOA *amoA* gene abundance. Sediment type was a major factor in determining both AOB *amoA* gene abundance and AOB community structure, possibly due to deeper oxygen penetration into the sandier sediments, increasing the area available for ammonia oxidation. Decreases in AOB *amoA* gene abundance were evident during summer and autumn, with maximum abundance and ammonia oxidation rates occurring in winter and early spring. PCR-DGGE of AOB *amoA* genes indicated that no seasonal changes to community composition occurred; however, a gradual movement in community composition occurred at 3 of the sites studied. The lack of correlation between AOA *amoA* gene abundance and ammonium oxidation rates, or any other environmental variable measured, may be related to the higher spatial variation amongst measurements, obscuring temporal trends, or the bimonthly sampling, which may have been too infrequent to capture temporal variability in the deposition of fresh organic matter. Alternatively, AOA may respond to changing substrate concentrations by an increase or decrease in transcript rather than gene abundance.

KEY WORDS: Coastal · Sediment · Ammonia oxidation · Archaeal *amoA* gene · Bacteria *amoA* gene

INTRODUCTION

Factors influencing the spatial and temporal patterns of marine nitrification and nitrifying microbes are poorly understood. Until recently, it was assumed that ammonia-oxidising bacteria (AOB) were solely responsible for the first step of nitrification. The AOB-centric viewpoint of ammonia oxidisation was challenged when genes similar to the ammonia monooxygenase genes of bacteria were discovered within archaeal scaffolds in both marine waters (Venter et al. 2004) and soils (Treusch et al. 2005, Leininger et al. 2006). Ammonia-oxidising archaea (AOA) 16S rRNA and *amoA* genes have now been detected in wastewater sludge (Mußmann et al. 2011), in coastal aquifers (Santoro et al. 2008) and within the marine environment in corals (Beman et al. 2007), sponges (Steger et al. 2008), sediments (Francis et al. 2005, Caffrey et al. 2007, Mosier & Francis 2008, Abell et al. 2010, Bernhard et al. 2010) and coastal and open waters (e.g. Francis et al. 2005, Wuchter et al. 2006, Beman et al. 2008).

*Corresponding author: ktait@pml.ac.uk

AOA consistently outnumber the AOB in pelagic systems (Coolen et al. 2007, Lam et al. 2007, Mincer et al. 2007, Bouskill et al. 2012, Horak et al. 2013), and there is substantial evidence to suggest that the AOA are the dominant nitrifiers in oceanic waters (Wuchter et al. 2006, Beman et al. 2008). However, the relative contribution of AOA and AOB to nitrification within sediments is less clear. The ratio of AOA:AOB appears to be highly variable with several studies reporting higher abundance of AOA *amoA* genes (Caffrey et al. 2007, Abell et al. 2010, Bernhard et al. 2010, Tait et al. 2014), whereas others have reported higher incidences of AOB relative to AOA *amoA* genes (Caffrey et al. 2007, Mosier & Francis 2008, Santoro et al. 2008, Wankel et al. 2011, Zheng et al. 2014). These differences in the relative abundance of AOA and AOB have been attributed to a number of factors, including salinity, temperature, ammonium concentration, dissolved oxygen, porewater sulphide concentrations and pH (Santoro et al. 2008, Abell et al. 2010, Biller et al. 2012, Bouskill et al. 2012, Dang et al. 2010, Tait et al. 2014). Salinity has been demonstrated to be a major factor influencing both nitrification rates (Seitzinger et al. 1991, Rysgaard et al. 1999), the abundance of AOA and AOB within sediments (Caffrey et al. 2007, Santoro et al. 2008, Bernhard et al. 2010) and the community structure of AOB (Francis et al. 2003, Bernhard et al. 2005, Mosier & Francis 2008, Bouskill et al. 2011, Jin et al. 2011) and AOA (Francis et al. 2005, Mosier & Francis 2008, Abell et al. 2010, Biller et al. 2012, Cao et al. 2013). For example, in a study of the relative abundance of AOA and AOB *amoA* genes in 6 different estuaries, Caffrey et al. (2007) reported abundance of AOA *amoA* genes to be positively correlated with salinity. In contrast, coastal aquifer sediment samples taken along a salinity gradient indicated AOB *amoA* gene abundance decreased with decreasing salinity, whereas AOA *amoA* gene copy numbers were relatively constant (Santoro et al. 2008). Biller et al. (2012) were able to show that 60% of the variation in aquatic AOA *amoA* sequence types corresponded to salinity. Although a high percentage, this highlights that additional environmental variables also significantly influence the distribution of AOA ecotypes in aquatic environments.

The contribution of AOA to nitrification, relative to the AOB, is also not well understood. For example, Caffrey et al. (2007) showed a significant relationship between potential nitrification rates and AOA *amoA* abundance in 2 out of 6 estuarine sediments but were unable to show any relationship with AOB *amoA* abundance. In contrast, the abundance of AOB *amoA* genes correlated with potential nitrification rates within estuarine sediments (Bernhard et al. 2010), whereas Magalhães et al. (2009) saw no correlation between AOB or AOA *amoA* abundance and nitrification potential flux in the intertidal sediments of the Douro River estuary in Portugal. Wankel et al. (2011) published similar results for sediments from the Elkhorn Slough, California, USA. Evaluating the relative contribution of AOA and AOB to ammonia oxidation is further complicated by the fact that recent evidence suggests that not all AOA are obligate chemolithoautotrophic ammonia oxidisers (Teira et al. 2006, Hatzenpichler et al. 2008, Mußmann et al. 2011) and that the AOA *AmoA* may have alternative substrates such as urea (Alonso-Sáez et al. 2012). In contrast, the chemoautotrophic nature of the AOB (Norton et al. 2008) indicates that their presence in the environment can be more confidently attributed to nitrification potential.

The link between AOA and AOB *amoA* gene abundance and nitrification rates was investigated in coastal marine sediments of the western English Channel. Four sites within the Western Channel Observatory (www.westernchannelobservatory.org.uk), chosen for their contrasting depth, sediment type and level of exposure to storm events, were sampled bimonthly between July 2008 and May 2011. Jennycliff (50° 20.91′ N, 04° 07.71′ W) and Cawsand (50° 19.81′ N, 04° 11.50′ W) represent shallow habitats (~10 m deep). Both sites are sheltered from the prevailing southwesterly winds, but they have different sediments types, with Jennycliff being coarse silt and Cawsand fine sand. Rame Mud (50° 17.75′ N, 04° 16.00′ W) and L4 (50° 13.30′ N, 04° 11.40′ W) are exposed sites with a depth of ~50 m, again with contrasting sediment type, Rame Mud being medium silt and L4 fine sand. The water column at the L4 station is also seasonally stratified from late-April until September (Smyth et al. 2010). Alongside collecting samples for DNA extraction and ammonia oxidation rate measurements, a whole suite of environmental variables were collected at the same time. Crucially, seabed salinity varies very little at each of these coastal sites. This provided the opportunity to survey the abundance and community composition of archaeal and bacterial ammonia-oxidiser abundance at each location over the 3 yr period and make use of the accompanying environmental measurements to identify key abiotic factors, other than salinity, driving AOA and AOB abundance in the sediments of the western English Channel.

This study examined the distribution of AOB and AOA in relation to temperature, sediment carbon and nitrogen content and nutrient concentrations,

taken from the bottom of the water column at the sediment surface. The abundance of both AOB and AOA was measured using quantitative PCR (qPCR) of archaeal- and bacterial-specific *amoA* gene PCR primers. Measurements of benthic nitrification rates were made at the same time. AOA and AOB community composition throughout the 3 yr period and at each location were compared using PCR-DGGE of *amoA* genes, and a small number of samples were also examined by DNA hybridisation to functional gene microarrays for the AOA (Bouskill et al. 2012) and the AOB (Ward et al. 2007, Bouskill et al. 2011).

MATERIALS AND METHODS

Site description and sampling protocols

Samples were taken approximately bimonthly from July 2008 to May 2011. Some winter sampling dates were missed due to adverse weather conditions, particularly at the furthest offshore site L4. Used in this analysis are the water depth of the site, sediment type (measured as specific surface area [SSSA]: Jennycliff = 3.95; Cawsand = 1.52; Rame Mud = 5.19 and L4 = 0.73 $m^2\ g^{-1}$), sediment carbon and nitrogen content and measurements of salinity, temperature and nutrients (ammonium, nitrate, nitrite, silicate and phosphate) taken from the bottom water. Details of methods can be found at www.westernchannelobservatory.org.uk, and data has been stored at the British Oceanographic Data Centre (www.bodc.ac.uk/). Porewater nutrients were not determined. However, as a first approximation, we calculated porewater NH_4^+ concentration in surficial sediment ($PWNH_4^+$; in the upper 1 cm of sediment where nitrification occurs) from the nutrient flux data and Fick's diffusion law:

$$PWNH_4^+ = \frac{Flux}{D \times \varphi} \times Dz + NH_4^+\ zero \qquad (1)$$

where 'Flux' was the ammonium flux calculated from nutrient flux experiments (data available from the British Oceanographic Data Centre www.bodc.ac.uk), '$NH_4^+{}_{zero}$' was the NH_4^+ concentration in overlying water at the start of nutrient flux experiments, '*Dz*' was the thickness of the diffusive layer (0.01 m), 'φ' was the porosity at each site and '*D*' was the diffusion coefficient for ammonium (9.85 $m^2\ d^{-1}$). *D* was taken from the apparent diffusion coefficients of NH_4^+ (Li & Gregory 1974), corrected for tortuosity (Sweerts et al. 1991). Although our approach is based on the assumption of diffusive flux (Fick's law), it implicitly considers bio-irrigation by using the measured 'Flux' data. The 'Flux' data carry an uncertainty of up to 40% based on replicate cores (SD of 8 cores).

Ammonia oxidation rate measurements

Ammonium oxidation rates were determined by slurry-type-incubations, *in vitro*, as previously described (Kitidis et al. 2011). Briefly, sediment for *in vitro* determination of ammonium oxidation was collected with a box core (0.25 m^2 surface area). Any overlying water was siphoned off, and surface sediment (top 1 cm) was scraped into 14 ml glass vials. Bottom water was added to each vial to a final ratio of approximately 2/3 surface sediment and 1/3 seawater. Triplicate slurries were treated either with allylthiourea (ATU) or sodium chlorate ($NaClO_3$) (0.1 ml of 0.1 mol l^{-1} added to each treatment). ATU is an inhibitor of the first stage of nitrification (i.e. ammonium oxidation) while $NaClO_3$ is an inhibitor of the second stage (NO_2^- oxidation). The vials were then sealed with rubber septa and incubated in the dark for 24 h at ambient seawater surface temperature (stored in a plastic box placed in a shaded tank with flowing surface water). At the end of each incubation, the supernatant in each vial was filtered (0.7 µM, Whatman GF/F) and the filtrate NO_2^- concentration was determined by manual colorimetric assay against $NaNO_2$ standards (Sigma; >99.9% purity; standard range: 0.0 to 2.0 µmol l^{-1}; $R^2 > 0.999$) (Grasshoff 1983). NH_3 oxidation rates were calculated as accumulation of NO_2^- in the $NaClO_3$ treatment compared to the ATU treatment. Post-incubation, the vials were dried and weighed in order to calculate the exact amount of sediment in each vial. The final NO_2^- concentration in each vial was normalised by the respective weight of sediment before rate calculations. The precision and detection limit of NO_2^- analysis were 5 and 9 nmol $NO_2^-\ l^{-1}$, respectively (initial NO_2^- concentration in all samples was >10 nmol l^{-1}). The corresponding limits of detection for rate calculations were 0.3 nmol $NH_4^+\ l^{-1}\ h^{-1}$ (ml wet $sediment^{-1}$)

DNA extraction

A multicorer was used to collect 8 replicate cores at Jennycliff, Rame Mud and L4, and a box corer was used to collect sediment at Cawsand. Surface sediment samples (1 ml) were taken using the barrel of a 2.5 ml syringe and immediately frozen at −20°C.

Sediment samples from 4 randomly selected cores were chosen for DNA extraction. Each sediment sample was homogenised by stirring with a sterile metal spatula and DNA extracted using the method of Laverock et al. (2010). Briefly, 0.5 g sediment was added to a sterile 2 ml microtube with 0.5 ml of 0.1 M sodium phosphate buffer (pH 8.0) and cells lysed by bead beating with 0.3 g each of 212 to 300 µm and 710 to 1180 µm glass beads (Sigma-Aldrich) and 0.5 ml phenol:chloroform:isoamyl alcohol (25:24:1, pH 8.0, Sigma-Aldrich). The lysate was separated from sediment by centrifugation, and the aqueous upper layer transferred to a clean 2 ml microtube containing 0.5 ml chloroform:isoamyl alcohol (24:1, Sigma-Aldrich), mixed and centrifuged again. The aqueous layer was purified by ethanol precipitation and resuspended in sterile water. DNA extracts then required further purification with the PowerClean® DNA Clean-Up Kit (Mobio) according to the manufacturer's instructions. Extraction of DNA was confirmed by agarose gel electrophoresis and quantified using a NanoDrop spectrophotometer (NanoDrop Technologies).

qPCR

An ABI 7000 sequence detection system (Applied Biosystems) and QuantiFast SYBR Green PCR Kit (Qiagen) were used for all qPCR experiments. To determine the abundance of archaeal and bacterial *amoA* genes, the following primers were used: arch-*amoA*F (5′-STA ATG GTC TGG CTT AGA CG-‘3) and arch-*amoA*R(5′-GCG GCC ATC CAT CTG TAT GT-3′) for archaeal *amoA* (Francis et al. 2005) and *amoA*1F (5′-GGG GTT TCT ACT GGT GGT-3′) and *amoA*2R (5′-CCT CKG SAA AGC CTT CTT C-3′) (Rotthauwe et al. 1997, Hornek et al. 2006) for bacterial *amoA* genes. For archaeal *amoA* genes, the 20 µl reaction mixture contained 10 µl of Master Mix, 300 nM of each primer and 10 ng of DNA, and PCR conditions were 5 min at 95°C followed by 40 cycles of 95°C for 15 s and 58.5°C for 1 min. For bacterial *amoA* genes, the 20 µl reactions contained 10 µl of Master Mix, 900 nM of each primer and 10 ng of DNA and PCR conditions were 5 min at 95°C followed by 40 cycles of 95°C for 15 s and 61.5°C for 1 min. Assays were conducted in triplicate and included a standard curve containing 10^2 to 108 amplicons μl^{-1} DNA. Standard curves for each primer pair were constructed using cloned sequences. Nucleic acids were quantified using a NanoDrop spectrophotometer (NanoDrop Technologies). Gene numbers were quantified by comparison to standard curves using the ABI Prism 7000 detection software. Automatic analysis settings were used to determine the threshold cycle (CT) values and baselines settings. The no-template controls were below the threshold in all experiments. For each standard curve, the slope, *y*-intercept, coefficient of determination (r^2) and the efficiency of amplification were determined. Values for archaeal *amoA* genes were typically: r^2 = 0.98, *y*-intercept = 40.78, E (amplification efficiency) = 86.32%, and for bacterial *amoA* genes: r^2 = 0.99, *y*-intercept = 34.33, E = 94.98%.

DGGE

DGGE analysis of archaeal and bacterial *amoA* gene sequences were performed with the INGENYphorU DGGE system (Ingeny). The primers used for the bacterial *amoA* qPCR were also used for DGGE analysis but with a base GC clamp (CGC CCG CCG CGC CCC GCG CCC GGC CCG CCG CCC CCG CCC C) attached to the 5′-end of the reverse primer. For archaeal *amoA*, PCR products were resolved without the requirement of a GC clamp. For both, the 50 µl PCR mixture contained 1 µl cDNA, 5× PCR buffer, 3.0 mM $MgCl_2$, 400 µM of each dNTP, 2.5 U GoTaq Flexi DNA Polymerase (Promega) and 100 nM of each primer and PCR conditions were as previously described (Shen et al. 2008). PCR products from the 4 replicate cores from each site were then combined to give one PCR product for each sampling time-point and the PCR products run on polyacylamide gradient gels with denaturing gradients of 35 to 55% for bacterial *amoA* and 10 to 50% for archaeal *amoA*. Gels were electrophoresed in 1× TAE (Tris-acetate-EDTA) at a constant temperature of 60°C for 16 h at 60 V. DGGE fingerprinting patterns were converted to presence/absence data using Gel Compar II software (Applied Maths) and the data imported into PRIMER v6 multivariate analysis software (Clarke & Gorley 2006) for statistical analysis.

Archaeal and bacterial *amoA* oligonucleotide probe design

This study employed the archaeal and bacterial *amoA* archetype arrays outlined by Ward & Bouskill (2011). The array employs an internal standard to filter and quantify signal intensity of the *amoA* probes.

Each 90-mer oligonucleotide probe contains a 70-mer bacterial- or archaeal-specific *amoA* archetype sequence combined with a 20-mer oligo (5′-GAT CCC CGG GAA TTG CCA TG-3′ for AOB *amoA* and 5′-GTA CTA CTA GCC TAG GCT AG-3′ for AOA *amoA*), functioning as an internal standard. The design and spotting of the *amoA* probes have been described previously (Ward & Bouskill 2011). For the AOA, 31 AOA archetype probes represent 1400 sequences taken from clone libraries built from terrestrial, aquatic and geothermal environments (Bouskill et al. 2012), and for the AOB, 28 individual probes represent 506 *amoA* sequences including both environmental and culture-based sequences (Bouskill et al. 2011).

amoA amplification, target preparation and microarray hybridization

Hybridization targets were produced from the PCR amplicons from Rame Mud and L4 in July 2008 and in March 2009 using methodology previously described (Ward & Bouskill 2011). PCR products from the 4 replicate cores from each site were then combined to give one PCR product for each sampling time-point. These were cleaned and labelled by incorporating amino-allyl-dUTP during linear amplification using Klenow enzyme. The Klenow product was purified and conjugated with Cy3 as described previously.

Cy3-labelled PCR product (200 ng) was combined with 2 × hybridization buffer (1 × final concentration; Agilent) and 0.25 pmol of a Cy5-labelled complementary 20-mer standard oligonucleotide and then incubated at 95°C for 5 min before being cooled to room temperature. Samples were hybridized to triplicate arrays by overnight incubation at 65°C and washed (Ward & Bouskill 2011). The arrays were scanned with an Agilent laser scanner (Agilent Technologies) and analysed using the Gene Pix Pro 6.0 software (Molecular Devices).

Various steps were employed to filter and quantify the signal hybridization data following Taroncher-Oldenburg et al. (2003). Signal hybridization intensities were standardized to the total fluorescence across the AOA or AOB probe sets to give a relative fluorescence ratio (RFR) allowing comparison between different arrays (Ward & Bouskill 2011). All of the original array files are available at GEO (Gene Expression Omnibus; www.ncbi.nlm.nih.gov/projects/geo/) at NCBI (National Centre for Biotechnology Information) under GEO Accession No. GSE50163.

Statistics

Analysis was performed using PRIMER v6 (Clarke & Gorley 2006) with the PERMANOVA+ add on (Anderson et al. 2008). Pearson's correlation coefficient was used to examine relationships among the abiotic variables, and also among the AOA and AOB *amoA* gene abundances and ammonia oxidation rates. Bray-Curtis resemblance matrices were used for gene and DGGE data throughout this study, whereas Euclidean distance similarity matrices were used for all process rate and environmental data. Two-way permutational multivariate analysis of variance (PERMANOVA), using site and month as fixed factors in a crossed design, were used to compare the effect of sediment location and season on the abundance of archaeal and bacterial *amoA* genes and ammonia oxidation rate data. For the presence/absence of DGGE banding patterns, resemblances between samples were generated using the Bray-Curtis coefficient, and non-metric multidimensional scaling (nMDS) ordinations were used to visualise the configuration of the different samples on a 2D scaling plot. The BIO-ENV routine (Clarke & Ainsworth 1993) within PRIMER was used to determine the environmental variables that best explained the variation in AOA and AOB *amoA* DGGE banding patterns and also in the *amoA* gene abundance data. The RELATE procedure, a non-parametric Mantel test, was used to test the hypothesis that the changes to the bacterial and archaeal *amoA* gene DGGE patterns varied linearly through time and also to assess relationships between the bacterial and archaeal *amoA* gene abundance data and the environmental variables.

RESULTS

Environmental variables

Environmental variables and statistical analyses for differences between sediment site and month are shown in Table 1. Salinity, measured in the bottom water at the sediment surface, was very similar at each of the 4 sites. The near-shore sites, particularly Jennycliff, experienced dips in salinity during periods of heavy rainfall (e.g. winter of 2010/2011), but these pulses of fresher water were not evident within the deeper waters at Rame Mud or L4 (Table 1). There was a clear seasonal signature to temperature and to the nutrients nitrite, nitrate, silicate and phosphate; concentrations of these nutri-

Table 1. Physical and chemical parameters measured at each site. Also included are the results of permutational multivariate analysis of variance (PERMANOVA) tests for the effect of sediment site and month on the environmental variables. Values are pseudo-*F*. Significance is indicated by ***p < 0.001, **p = 0.01 and *p = 0.05. TC, TOC and TIC are total carbon, total organic carbon and total inorganic carbon, respectively. TN, TON, TIN are total nitrogen, total organic nitrogen and total inorganic nitrogen, respectively

Site	Year	Month	CTD (bottom water column)		Sediment C and N content							Bottom water column nutrients (µM)					Porewater (µM)
			Temp.	Salinity	TC	TOC	TIC	TN	TON	TIN	C:N	NO_2^-	NO_3^-	NH_4^+	SiO_3^{2-}	PO_4^{3-}	NH_4^+
All sites	PERM-ANOVA	Site	0.186	0.834	29.98***	10.97***	7.55***	12.79***	7.99***	8.5**	8.53***	0.415	3.59*	0.749	2.21	0.357	4.2*
		Month	31.18***	0.635	1.31	2.87*	2.88*	1.74	0.479	6.39**	2.64*	9.9***	33.7***	1.35	23.6***	5.24*	1.1
		Si × Mo	0.379	0.734	1.1	0.974	1.75	0.8	0.47	1.72	1.05	0.8	1.57	2.53*	1.48	0.2548	1.52
Jenny-cliff	2008	July	13.25	35.82	3.57	0.93	2.63	0.09	0.05	0.04	39.63	0.08	0.74	0.03	0.52	0.10	4.28
		Sep			3.15	0.47	2.68	0.07	0.04	0.03	44.50	0.30	5.03	1.09	3.00	0.29	5.25
		Nov										0.84	8.63	1.52	6.50	0.44	3.9
	2009	Jan	8.79	34.67								0.22	12.60	0.43	5.88	0.40	1.27
		Mar	8.42	34.59	3.83	1.20	2.63	0.14	0.09	0.05	27.72	0.25	9.82	0.99	6.31	0.72	2.09
		May			4.05	1.97	2.08	0.18	0.12	0.06	22.26	0.09	2.55	0.65	2.02	0.15	4.59
		July	11.50	35.09	4.35	1.51	2.84	0.17	0.12	0.05	25.89	0.05	0.32	0.49	1.08	0.10	2.92
		Sep	15.01	34.81								0.37	3.42	0.64	4.96	0.39	2.01
		Nov	14.52	34.16								0.43	7.85	1.49	6.54	0.54	3.71
	2010	Jan	7.91	34.52	3.60	1.16	2.44	0.16	0.10	0.06	22.94	0.37	12.28	1.36	6.69	2.82	4.32
		Mar	8.02	34.80	3.65	1.57	2.09	0.19	0.14	0.06	19.13	0.25	8.18	0.50	4.06	0.61	2.2
		May	10.27	34.87	3.94	0.89	3.05	0.09	0.05	0.04	45.61	0.04	1.07	0.61	1.50	0.16	3.11
		July	14.99	34.74	3.27	0.92	2.35	0.10	0.07	0.03	31.34	0.02	0.13	0.38	0.93	0.14	3.26
		Sep	16.16	34.75	3.79	0.75	3.03	0.10	0.05	0.05	38.89	0.13	1.22	0.99	2.43	0.23	2.2
		Nov	13.64	33.51	2.98	0.71	2.27	0.08	0.06	0.02	37.74	0.77	10.67	3.43	6.96	0.65	5.37
	2011	Jan															
		Mar	9.97	33.93	3.43	1.01	2.42	0.10	0.06	0.04	34.72	0.13	9.55	1.29	4.24	0.56	1.99
		May	11.58	35.08	3.02	0.15	2.87	0.06	0.04	0.02	50.29		0.38	0.54	1.78	0.20	0.93
Caw-sand	2008	July	13.69	35.18	2.81	0.81	2.00	0.07	0.04	0.02	43.20	0.04	0.15	0.03	0.59	0.07	2.45
		Sep			2.91	0.60	2.31	0.06	0.05	0.01	46.05	0.31	2.16	0.55	2.02	0.16	2.37
		Nov										0.79	17.22	1.99	9.83	0.74	4.15
	2009	Jan	8.51	34.65	2.70	0.59	2.11	0.04	0.02	0.02	67.92	0.20	9.67	0.33	6.41	0.78	3.03
		Mar	8.51	34.70	2.55	0.03	2.51	0.12			21.58	0.21	15.77	1.07	7.79	0.61	1.18
		May	11.42	35.08								0.08	1.32	0.60	1.94	0.15	
		July			3.01	0.94	2.07	0.15	0.10	0.05	19.93	0.10	1.44	0.77	1.61	0.12	2.73
		Sep	14.30	34.96	2.43	0.22	2.21	0.06	0.03	0.03	40.24	0.32	2.26	0.93	5.11	0.39	4.9
		Nov			2.74	0.42	2.32	0.09	0.05	0.04	32.24	0.36	7.40	0.65	5.88	0.49	8.6
	2010	Jan	7.95	34.73	2.46	0.33	2.13	0.07	0.02	0.04	37.88	0.38	11.23	0.52			8.75
		Mar	7.93	34.93	2.55	0.61	1.93	0.12	0.08	0.03	22.14	0.29	8.56	0.39	4.23	0.61	7.68
		May	10.69	4.36	2.86	0.57	2.30	0.05	0.04	0.02	52.28	0.04	0.58	0.23	0.84	0.13	1.89
		July	13.72	35.01	2.55	0.50	2.06	0.05	0.02	0.03	51.03	0.03	0.45	0.59	1.56	0.15	12.92
		Sep	16.05	34.97	2.71	0.65	2.06	0.06	0.04	0.02	41.90	0.16	0.43	0.91	2.24	0.26	0.86
		Nov	13.97	34.75	2.87	0.38	2.50	0.04	0.02	0.02	73.63	0.62	5.51	0.85	4.23	0.43	9.21
	2011	Jan															
		Mar	8.75	35.00	2.65	0.31	2.34	0.05	0.03	0.02	55.05	0.09	6.25	0.59	3.04	0.38	4.27
		May	11.50	35.17	2.79	0.32	2.47	0.04	0.02	0.02	75.20		0.24	0.12	1.43	0.16	0.64

Table 1 (continued)

Site	Year	Month	CTD (bottom water column)		Sediment C and N content							Bottom water column nutrients (µM)					Porewater (µM)
			Temp.	Salinity	TC	TOC	TIC	TN	TON	TIN	C:N	NO_2^-	NO_3^-	NH_4^+	SiO_3^{2-}	PO_4^{3-}	NH_4^+
All sites	PERM-ANOVA	Site	0.186	0.834	29.98***	10.97***	7.55***	12.79***	7.99***	8.5**	8.53***	0.415	3.59*	0.749	2.21	0.357	4.2*
		Month	31.18***	0.635	1.31	2.87*	2.88*	1.74	0.479	6.39**	2.64*	9.9***	33.7***	1.35	23.6***	5.24*	1.1
		Si × Mo	0.379	0.734	1.1	0.974	1.75	0.8	0.47	1.72	1.05	0.8	1.57	2.53*	1.48	0.548	1.52
Rame Mud	2008	July	12.58	35.28	3.12	2.30	0.82	0.10	0.02	0.08	30.23	0.21	1.56	1.19	2.65	0.28	0.9
		Sep	14.65	35.15	3.40	1.07	2.33	0.14	0.09	0.04	24.99	0.50	4.51	4.33	5.26	0.47	3.87
		Nov	13.20	35.09								0.87	5.49	0.79	4.34	0.39	3.07
	2009	Jan	8.90	34.99	3.88			0.20			19.87	0.19	9.47	0.03	5.48	0.47	1.85
		Mar	8.78	35.08	3.55	0.82	2.73	0.07	0.04	0.03	49.39	0.32	6.30		4.08	0.42	1.92
		May	12.96	35.21	3.80	0.92	2.88	0.08	0.04	0.04	49.39	0.05	0.53	1.06	1.84	0.28	3.56
		July	13.15	35.26	3.74	1.45	2.30	0.26	0.17	0.08	14.56		0.02	0.34	0.44	0.04	2.62
		Sep	15.62	35.16	3.27	0.98	2.30	0.14	0.12	0.02	23.40	0.73	1.58	0.49	3.63	0.21	2.52
		Nov			3.42	1.34	2.09	0.19	0.15	0.03	18.49	0.08	7.57	0.07	4.51	0.56	3.07
	2010	Jan	8.70	35.04	3.42	1.22	2.20	0.20	0.14	0.06	17.12	0.17	8.47	0.30	5.02	2.65	2.74
		Mar	7.93	35.16	3.12	0.92	2.20	0.15	0.12	0.03	20.51	0.27	6.69	0.44	3.61	0.58	2.27
		May	9.79	35.10	3.51	0.73	2.78	0.13	0.08	0.05	27.90		0.03	0.49	1.05	0.19	3.74
		July	11.76	35.13	3.14	0.75	2.39	0.12	0.09	0.04	25.42	0.01	0.33	2.11	2.97	0.28	
		Sep	14.29	35.26	3.26	0.55	2.71	0.13	0.11	0.02	25.05	0.20	0.36	1.19	2.61	0.20	2.01
		Nov	13.01	35.21	2.85	0.49	2.36	0.09	0.06	0.03	32.85	0.11	5.24	0.15	4.47	0.45	1.04
	2011	Jan															
		Mar	8.62	35.20	2.95	0.88	2.07	0.09	0.06	0.03	33.49	0.11	5.20	0.52	3.02	0.38	0.85
		May	11.27	35.23	3.13	0.49	2.64	0.10	0.07	0.03	30.17	0.05	0.63	0.99	2.59	0.23	2.21
L4	2008	July	12.98	35.26								0.19	1.24	0.55	1.69	0.20	35.33
		Sep	14.16	35.22	2.32	0.19	2.13	0.03	0.02	0.02	72.61	0.38	5.16	1.05	4.15	0.48	2.32
		Nov	13.29	35.17	2.88	0.50	2.38	0.11	0.08	0.03	26.22	0.69	2.79	1.17	3.14	0.30	4.45
	2009	Jan															
		Mar			2.22	0.15	2.07	0.03	0.01	0.01	83.51	0.22	6.59		3.66	0.54	2.15
		May	11.85	35.27	2.33	0.40	1.93	0.03	0.01	0.01	83.63	0.06	0.38	1.69	1.67	0.18	3.6
		July	12.77	35.27	2.48	0.49	1.99	0.09	0.03	0.05	28.83	0.04	0.68	1.90	1.94	0.22	6.54
		Sep	13.95	35.24	2.29	0.36	1.93	0.03	0.02	0.01	83.80	0.24	5.64	0.07	4.62	0.29	2.91
		Nov											0.00				0.95
	2010	Jan	9.09	35.19	2.12	0.34	1.79	0.06	0.03	0.03	36.60	0.23	6.77	0.16	4.39	2.21	1.39
		Mar	8.01	35.17	1.86	0.49	1.37	0.07	0.04	0.04	26.51	0.24	7.16	0.24	3.62	0.55	4
		May	9.57	35.12										0.41	1.20	0.20	5.59
		July	11.76	35.13	2.48	0.36	2.12	0.02	0.02	0.01	105.84	0.04	1.13	3.09	2.28	0.28	
		Sep	14.29	35.26								0.23	3.92	0.36	2.38	0.37	2.15
		Nov	13.01	35.21	2.75	0.60	2.16	0.03	0.02	0.01	101.07	0.09	5.09	0.20	4.13	0.43	2.6
	2011	Jan															
		Mar	8.62	35.20	2.53	0.26	2.27	0.03	0.02	0.01	100.78	0.14	6.42	0.68	3.42	0.48	3.66
		May	11.12	35.25	2.55	0.49	2.06	0.03	0.02	0.01	79.81	0.05	0.63	1.20	2.43	0.25	

ents are higher in winter months (Table 1). Ammonium concentrations revealed a more complex pattern and were highly variable seasonally and between the different sites: at the shallow sites, ammonium concentration peaked in November, whereas at the deeper sites stratification coincided with peaks in ammonium concentration during summer months (Table 1). Porewater NH_4^+ was 1 to 2 orders of magnitude higher than in the overlying water column, driving a consistent efflux of ammonium from the sediments. Sediment type was related to carbon and nitrogen content, both of which were higher at the muddy sites than the sandier sites (Table 1). There was also some evidence for seasonal fluctuations in the organic and inorganic carbon and inorganic nitrogen content of the sediments, which tended to decrease during summer and autumn months (Table 1).

Ammonia oxidation rates measurements

Comparisons of ammonia oxidation rates, measured from each sediment site from July 2008 to May 2011, revealed a strong influence of sediment type, with higher rates of ammonia oxidation occurring in the sandier sediments (Cawsand and L4) than in the muddy sediments (Jennycliff and Rame Mud) (Fig. 1A–D). For Cawsand and L4, average ammonia oxidation rates of 18.2 (±6.8 SD) and 29.7 (±10.8 SD) nmol l^{-1} h^{-1} ml^{-1} wet sediment were recorded, respectively, whereas Jennycliff and Rame Mud average rates were 7.7 (±6.3 SD) and 12 (±5.4 SD) nmol l^{-1} h^{-1} ml^{-1} wet sediment, respectively. PERMANOVA tests performed on Euclidean distance matrices derived from the ammonia oxidation rate data confirmed the significant differences between sites (F = 2.895; p = 0.042), but no seasonal differences were detected (F = 1.986; p = 0.113). However, although not regular in occurrence, peaks in activity tended to occur within January, March and May for Jennycliff, Cawsand and Rame Mud, whereas peaks at L4 were less regular, with large peaks in May 2009 and November 2010 (Fig. 1A–D). Particularly high ammonia oxidation rates were also recorded at Cawsand in January 2009 (92.7 nmol l^{-1} h^{-1} ml^{-1} wet sediment). Pearson's correlation coefficients were calculated for the ammonia oxidation rate measurements and the environmental variables (see Table 1A in the Appendix) to determine possible relationships between the rate data and environmental measurements, but no significant correlations were found.

AOB and AOA *amoA* gene abundance

For each sample, the abundance of AOB (Figs. 1A–D) and AOA (Fig. 1E–H) was measured by quantification of the respective *amoA* genes. The abundance of AOB *amoA* genes strongly differed between sites (PERMANOVA F = 44.597; p < 0.001). Abundance was higher at the sandier sediment sites Cawsand (averaging 2.76×10^6 [$\pm 9.78 \times 10^5$ SD] copies g^{-1} sediment) and L4 (6.95×10^6 [$\pm 1.85 \times 10^6$ SD] copies g^{-1} sediment), and lower at the muddy sediment sites Jennycliff (averaging 1.71×10^6 [$\pm 7.5 \times 10^5$ SD] copies g^{-1} sediment) and Rame Mud (1.16×10^6 [$\pm 4.37 \times 10^5$ SD] copies g^{-1} sediment) (Fig. 1A–D). As evident by the lower F-ratio, seasonal changes to AOB *amoA* abundance were less pronounced than the site-specific differences (Fig. 1A–D; PERMANOVA F = 5.037; p < 0.001), with increases in abundance generally occurring in January, March and May at all 4 sites, with additional peaks in September in Cawsand sediments (Fig. 1A–D).

AOA *amoA* genes were more abundant than AOB *amoA* genes at each site: ratios of AOA:AOB *amoA* gene abundance averaged for each site were 5.1 (±2.76 SD) for Jennycliff, 4.87 (±6.07 SD) for Cawsand, 10.8 (±5.77 SD) for Rame Mud, and 1.83 (±1.46 SD) for L4. AOA *amoA* gene abundance also differed between sites, but as evident from the lower F-ratio, not to the same extent as AOB *amoA* abundance (Fig. 1E–H; PERMANOVA F = 3.881; p < 0.001). Average abundance was 6.96×10^6 ($\pm 3.55 \times 10^6$ SD) gene copies g^{-1} sediment at Jennycliff, 6.62×10^6 ($\pm 3.21 \times 10^6$ SD) at Cawsand, 1.10×10^7 at Rame Mud ($\pm 4.54 \times 10^6$ SD) and 1.19×10^7 ($\pm 6.81 \times 10^6$ SD) at L4. These differences in abundance could be attributed to the unusually high peaks in abundance in March and May at Rame Mud in 2009 and in July and September in the same year at L4. However, AOA *amoA* abundance was also higher (average of 2.31×10^6 [$\pm 5.22 \times 10^6$ SD] AOA *amoA* gene copies g^{-1} sediment) at the deeper sites than the shallow sites at all the other times. There was also evidence of seasonal differences in AOA *amoA* abundance

Fig. 1. Spatial and temporal changes to the abundance g^{-1} sediment of bacterial and archaeal *amoA* genes and ammonia oxidation rates (▲). To highlight their close relationship, bacterial *amoA* gene abundance (□) and ammonia oxidation rate measurements are plotted together for (A) Jennycliff, (B) Cawsand, (C) Rame Mud and (D) L4, and (●) archaeal *amoA* gene abundance measurements plotted separately for (E) Jennycliff, (F) Cawsand, (G) Rame Mud and (H) L4. Four replicate core samples were used for each measurement and error bars are standard deviation (n = 4)

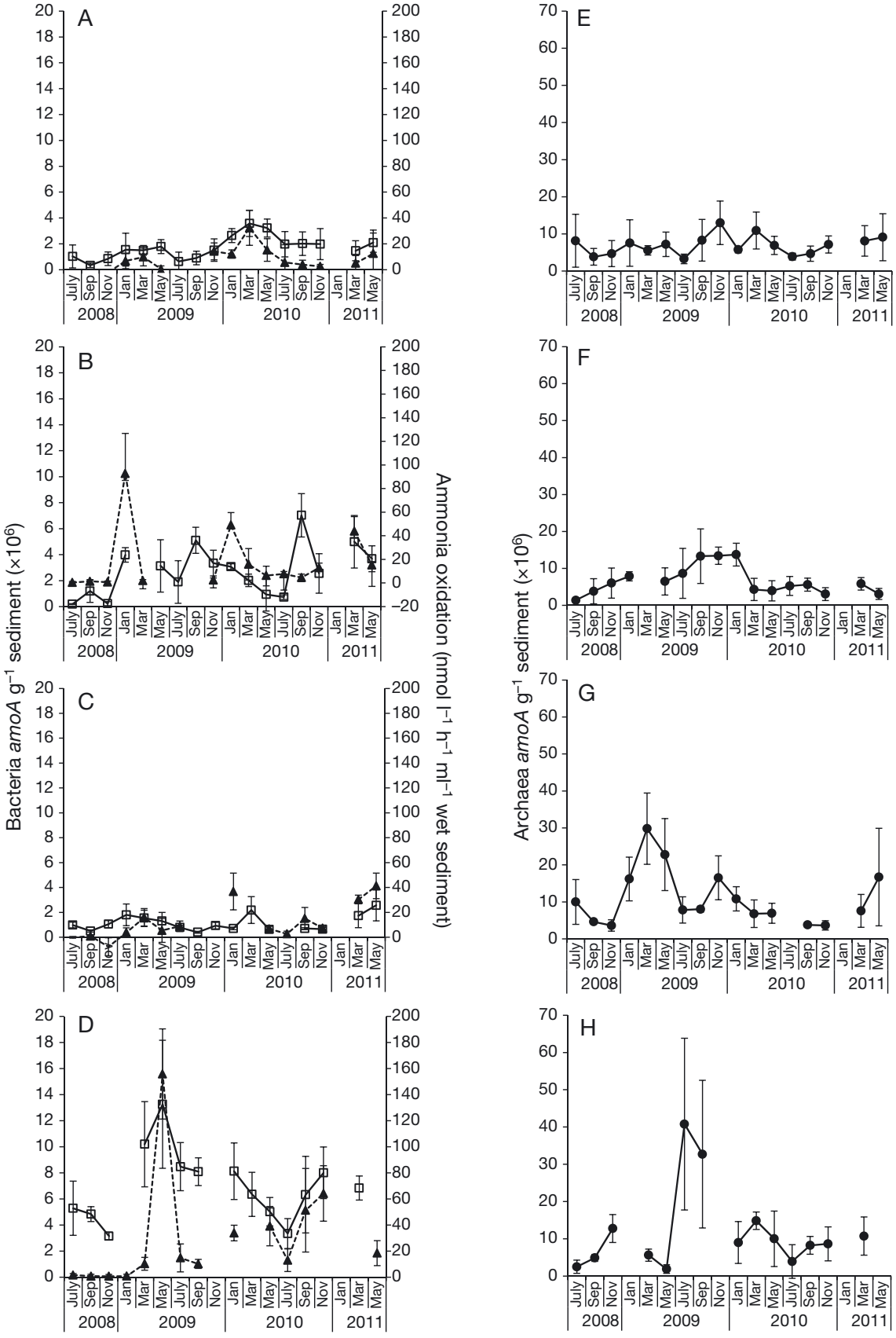
A
B
C
D
E
F
G
H
Bacteria amoA g−1 sediment (×10^6)
Ammonia oxidation (nmol l−1 h−1 ml−1 wet sediment)
Archaea amoA g−1 sediment (×10^6)
July Sep Nov Jan Mar May July Sep Nov Jan Mar May July Sep Nov Jan Mar May
2008 2009 2010 2011

(Fig. 1E–H; PERMANOVA $F = 2.74$; $p = 0.004$), but a significant interaction (PERMANOVA $F = 1.923$; $p = 0.004$) indicates that seasonal changes to the abundance of AOA *amoA* genes differed among sites (Fig. 1E–H). Aside from the unusually high peaks in abundance at L4 in July and September of 2009 (Fig. 1H), AOA *amoA* abundance tended to be at its lowest in July and September (Fig. 1E–G).

There was a significant correlation between ammonia oxidation rates and AOB *amoA* gene abundance ($\rho = 0.565$; $p < 0.001$), but not AOA *amoA* gene abundance ($\rho = 0.003$; $p = 0.981$). AOB *amoA* gene abundance appeared to be more variable at Cawsand, and the relationship between gene abundance and ammonia oxidation rates less clear (Fig. 1B): correlation between AOB *amoA* gene abundance and ammonia oxidation was higher when the Cawsand samples were removed from the analysis ($\rho = 0.608$; $p < 0.001$).

RELATE tests comparing a Euclidean distance matrix of the AOB *amoA* gene abundance and the Euclidean distance matrix of the $\log(x + 1)$-transformed, normalised environmental data indicated a significant relationship between the 2 datasets ($\rho = 0.352$; $p < 0.001$). To further examine the environmental factors driving variation in AOB *amoA* gene abundance, a BEST analysis using the BIO-ENV procedure (Clarke & Ainsworth 1993) was performed. The variables best explaining the variation in AOB *amoA* gene abundance data were the ammonia oxidation rate and sediment particle size ($\rho = 0.526$; $p < 0.001$). This verifies the correlation between the AOB and ammonia oxidation and also confirms a preference of the AOB for sandier sediments as indicated by the AOA:AOB *amoA* gene abundance ratios. The sandier sediments had lower carbon and nitrogen content compared to the muddier sediments. Although inclusion of organic carbon within the correlation analysis also produced a significant result ($\rho = 0.479$; $p < 0.001$), this value was lower than the correlation coefficient for AOB *amoA* gene abundance with sediment mean specific surface area and ammonia oxidation alone, indicating that it was likely the sediment particle size rather than organic carbon content that was a key factor in determining AOB abundance and activity.

In contrast, RELATE tests for a possible relationship between a Euclidean distance matrix of the AOA *amoA* gene abundance data and the environmental variables found no evidence for a significant relationship ($\rho = 0.061$; $p = 0.137$). Similarly, BEST analyses failed to identify any environmental variable which could explain the changes to AOA *amoA* gene abundance.

AOB *amoA* community composition

Comparisons of AOB community composition at each of the 4 sediment sites were first studied using PCR-DGGE of the AOB *amoA* gene. The PCR-DGGE picked up a high number of bands: a total of 56 unique bands were detected on the DGGE gels, with between 40 and 46 bands per sediment site. Analysis of the DGGE banding patterns indicated that the AOB *amoA*-based communities differed between sites (Fig. 2A) (PERMANOVA $F = 14.606$; $p < 0.001$). Further comparison of the AOB *amoA* communities at each site using post hoc tests revealed the nearshore sites at Jennycliff and Cawsand had similar DGGE patterns of AOB *amoA* gene ($t = 1.2298$; $p = 0.157$). There was no evidence of any seasonal patterns to the DGGE analysis of the AOB *amoA* genes at each site (PERMANOVA $F = 0.77634$; $p = 0.789$). However, RELATE tests for seriality indicate that the communities gradually shifted through the 3 yr period studied at Jennycliff ($\rho = 0.504$; $p < 0.001$), Cawsand ($\rho = 0.459$; $p = 0.002$) and Rame Mud ($\rho = 0.479$; $p = 0.002$), but not L4 ($\rho = 0.066$; $p = 0.255$). The gradual shift in AOB *amoA* gene-based community composition at Jennycliff, Cawsand and Rame Mud can be seen in Fig. 2C,D.

To identify the environmental variables that influenced the differences in community composition, a BEST analysis was conducted to find which subset of measured environmental variables and the ammonia oxidation rates best matched the AOB *amoA* gene DGGE Bray-Curtis resemblance matrix used to generate the MDS plot in Fig. 2A. This indicated that sediment particle size and depth of the water column were the variables best explaining the AOB *amoA* community pattern seen in Fig. 1A ($\rho = 0.664$; $p = 0.01$).

Community composition of the AOB within 4 sediments samples (Rame Mud in July 2008 and March 2009 and L4 in July 2008 and March 2009) was also investigated using a functional gene microarray composed of AOB *amoA* archetype probes (Fig. 3A). These samples are highlighted on the MDS plot in Fig. 2A. Hybridization signals averaged from replicate arrays are expressed as relative fluorescence ratios (RFRs) to indicate relative abundance of the 28 archetypes, representative of all known AOB clades at the time the array was designed (Bouskill et al. 2011). This revealed a dominance of coastal sediment clades at both these sites (Fig. 3A): the strongest hybridization signals on the AOB array were for archetypes A1 and A5. A1 represents the main marine *Nitrosospira* clade, derived from se-

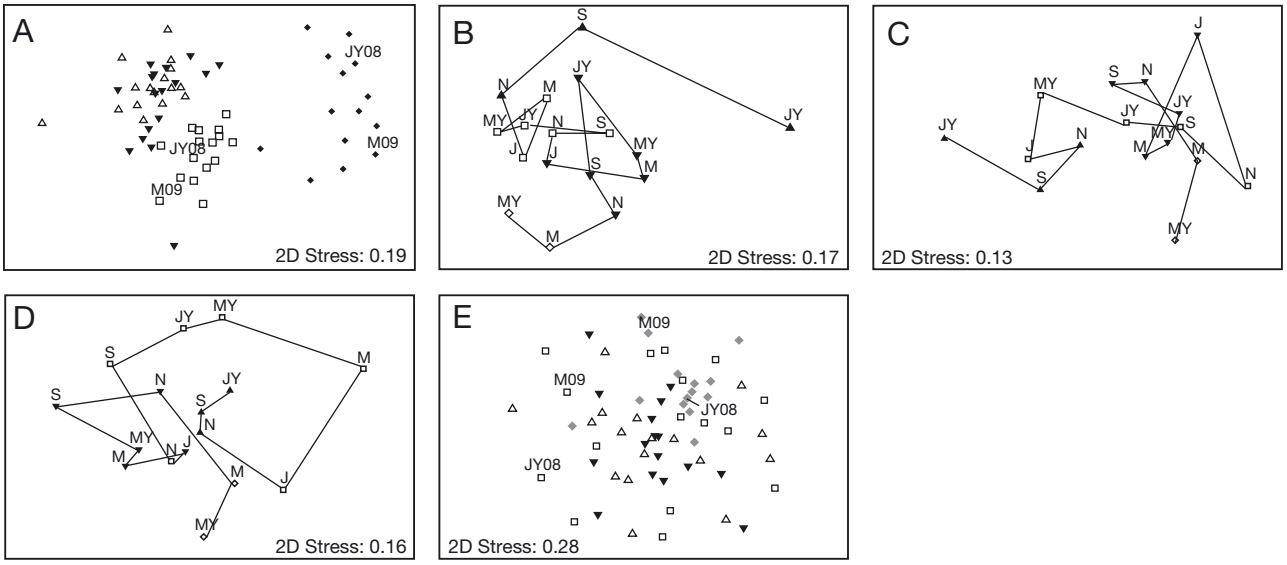

Fig. 2. Non-metric multidimensional scaling (nMDS) ordination of Bray-Curtis resemblances calculated from DGGE band presence/absence, illustrating spatial differences in (A) bacterial and (E) archaeal *amoA* genes. Symbols refer to sediment site: Jennycliff (△), Cawsand (▼), Rame Mud (□) and L4 (◆). Also indicated are samples used for the *amoA* gene microarray analysis. For clarity, ammonia-oxidising archaea (AOA) *amoA* data points for L4 are highlighted in grey. Also shown are the gradual shift in ammonia-oxidising bacteria (AOB) *amoA* genes through time at the (B) Jennycliff, (C) Cawsand and (D) Rame sites. Symbols refer to year sampled (2008, ▲; 2009, □; 2010, ▼; 2011, ◇) and letters refer to month: (JY) July; (S) September; (N) November; (J) January; (M) March and (MY) May

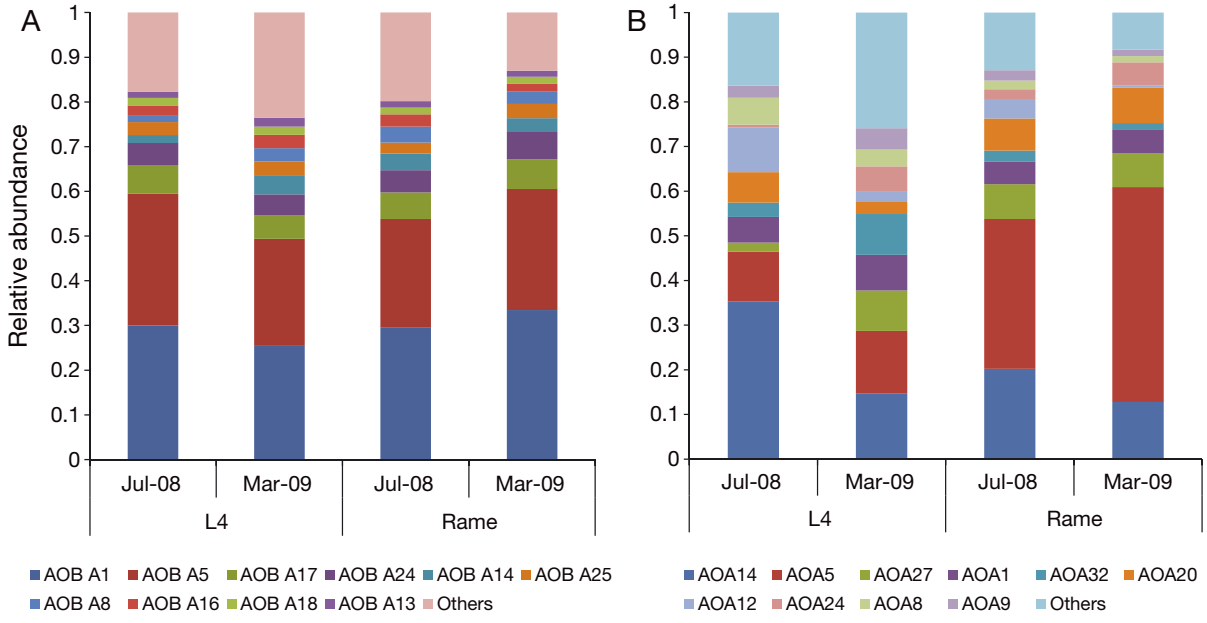

Fig. 3. Top 10 most abundant relative fluorescence ratios (RFRs) for (A) ammonia-oxidising archaea (AOB) and (B) ammonia-oxidising bacteria (AOA) *amoA* archetype probes from Rame Mud and L4 samples taken in July 2008 and March 2010. Details of probes for the archaeal and bacterial *amoA* archetypes can be found at Bowen et al. (2013)

quences originally obtained from coastal regions of the US east and west coasts, whereas A5 represents a smaller group of distinct sequences from the same regions. Neither of these has cultured representatives. Archetype A17, derived from sequences including the cultured species *Nitrosomonas ureae* as well as a few related environmental sequences and A24, based solely on the cultured species *Nitrosococcus halophilus*, also produced significant signals. An archetype representing *N. aestuarii* and related environmental sequences (A10) was a very minor component in these samples and other estuarine types (e.g. A16 and 14) were present, but in small quantities. Unlike the PCR-DGGE data, all 4 samples had very similar array profiles: paired *t*-tests for differences among sites or months all failed to indicate significant differences (results not shown).

AOA *amoA* community composition

Comparisons of AOA *amoA*-based community composition at each of the 4 sediment sites using PCR-DGGE also indicated differences amongst the AOA *amoA*-based communities (PERMANOVA F = 14.606; $p < 0.001$). Post hoc analysis to further compare the AOA *amoA* community profiles indicated that this was mainly driven by differences between L4 and the other 3 sites: the other 3 sites were similar to each other (i.e. ρ values for differences between L4 and Jennycliff, L4 and Cawsand, and L4 and Rame Mud were all $p < 0.001$, whereas Jennycliff and Cawsand $p = 0.108$; Jennycliff and Rame Mud $p = 0.08$, and Cawsand and Rame Mud $p = 0.01$). The difference in DGGE banding patterns at L4 and at the other sites has been highlighted in Fig. 2C. Again, a high number of unique bands were identified within the dataset (81) with a slightly lower number of unique bands evident for L4 (66) than the 3 other sites (75–76). Similar to the AOB *amoA* gene PCR-DGGE data, there was no evidence of seasonal changes to the AOA *amoA* genes (PERMANOVA F = 0.973; $p = 0.541$); however, unlike the AOB *amoA* gene analysis, RELATE tests for seriality indicated no gradual shifts to the community composition through time. BIO-ENV tests to identify environmental variables contributing to the AOA *amoA* community pattern seen in Fig. 2C also failed to detect any significant relationships.

The AOA *amoA* array data indicated the community was dominated by a few prominent signals (e.g. AOA14 and AOA5), which were highly reproducible (Fig. 3B). The minor constituents (e.g. AOA1, AOA20 and AOA27) were more variable (SD up to 10% among replicates), but they contribute far less to the overall comparison among samples. AOA5 was derived from estuarine sediment sequences, including a large number of sequences from Bahia del Tobari, a marginal estuary in the Gulf of California with full strength seawater salinity and high nutrient levels. AOA14 represents a few Tobari sequences and several sequences derived from coral tissues (Beman et al. 2007). AOA1 was based on a large number of environmental sequences and includes *N. maritimus*, the most commonly detected clade in current marine databases. AOA20 and AOA27 were detected from sequences from coral and California beach sediments respectively. Paired *t*-tests indicated that the L4 sediment sample differed from the Rame Mud sediment sample in March 2009 ($t = 4.71$; $p < 0.001$), but not in July ($t = 1.73$; $p = 0.094$). Significant differences in community composition were also seen when the Rame Mud sediments and L4 sediments sampled in July 2008 and March 2009 were compared ($t = 316$; $p = 0.004$ and $t = 2.33$; $p = 0.027$, respectively). For example, Rame Mud sediments produced a substantially higher signal for AOA5 and AOA27 than the L4 samples. In contrast to the AOA PCR-DGGE data, this indicates a shift in community composition occurred between July 2008 and March 2009.

DISCUSSION

Similar to previous studies of benthic estuarine and coastal environments (Caffrey et al. 2007, Mosier & Francis 2008, Santoro et al. 2008, Moin et al. 2009, Abell et al. 2010, Bernhard et al. 2010), the current study found the *amoA* genes of the AOA to be higher in abundance than the AOB *amoA* genes (Fig. 1). It is also evident that the gene abundances reported here fit within the ranges of previously reported values for these genes within similar sediment environments (10^5–10^7 for AOB and 10^6–10^7 *amoA* genes g^{-1} sediment for AOA; Caffrey et al. 2007, Abell et al. 2010, Bernhard et al. 2010) and from a study comparing AOA and AOB *amoA* gene abundance in surface sediments and burrows of the burrowing shrimp *Upogebia deltaura* in Jennycliff mud (Laverock et al. 2014). However, despite the higher abundance of AOA within each of the sediments examined, there was a significant correlation between the ammonia oxidation rate and AOB *amoA* gene abundance data, but not between the ammonia oxidation rate and AOA *amoA* gene abundance data.

Along with ammonia oxidation rate, sediment particle size was the only variable that correlated with the spatial and temporal patterns of AOB *amoA* gene abundance; this implies a preference of the AOB for the larger sediment particles at Cawsand and L4. This may be due to increased oxygen penetration into the sandier sediments which will increase the thickness, and by extension volume, of the sediment layer where nitrification can occur. Alternatively, high sulphide concentrations, produced by the action of anaerobic sulphate and sulphur reducing bacteria within sediments, are known to inhibit nitrification (Joye & Hollibaugh 1995, Caffrey et al. 2007). Visual inspection of the Jennycliff and Rame Mud sediments suggested anoxia as these turned black within 1 to 3 cm of the sediment surface; this was not evident at Cawsand or L4.

Also apparent were seasonal changes to the abundances of AOB *amoA* genes: numbers were higher within winter months and, although not statistically significant, the same patterns were evident for the ammonia oxidation rates (Fig. 1). However, the cause of these decreases during summer months was not clear. Similar decreases to nitrification during summer months have been observed in a number of benthic studies (Hansen et al. 1981, Seitzinger et al. 1991, Thompson et al. 1995, Eriksson et al. 2003, Bernhard et al. 2007). A combination of factors may cause this seasonal dip in nitrification. For example, it would be expected that the seasonal changes to ammonia oxidation be related to changing substrate availability. Yet, there was no correlation between our measurements of porewater ammonium. It is possible that our calculated porewater ammonium is not an accurate representation of *in situ* concentrations. In our calculations, we assume a diffusive efflux which is not moderated by uptake, either through nitrification or by microphytobenthos in the shallower sites. Our porewater ammonium may, thus, be underestimated. Previous work has also shown nitrification in Saanich Inlet, British Columbia, Canada, to be independent of ammonia concentration in the range of 0.2 to 62 µmol l^{-1} (Ward & Kilpatrick 1990). Assuming that benthic microbes have a similarly high affinity for ammonium, it is conceivable that nitrifiers in this study do not experience ammonium limitation. In a study of Elkhorn Slough sediments, potential nitrification rates only positively correlated with porewater ammonium concentrations when oxygen concentrations were sufficiently high for nitrification to occur. Although the stimulation of phytoplankton growth during summer months, and the subsequent deposition of this material onto the sediment floor either from the aggregation and sinking of phytoplankton or plankton detritus, leads to higher mineralisation rates and consequently higher ammonium concentrations, the resultant increased growth of heterotrophic microbes is thought to outcompete nitrifiers for oxygen, and this is thought to cause a decrease in nitrification during summer months (Hansen et al. 1981, Risgaard-Petersen et al. 2004). Unfortunately, bottom water oxygen data is only available from the L4 site from July 2009 onwards (www.westernchannelobservatory.org.uk/data.php). However, this data does indicate considerable oxygen depletion occurs at depth following phytoplankton blooms. In some cases, temporal changes to nitrification have been linked to blooms of microphytobenthos, which outcompete nitrifiers for ammonium during the day and limit O_2 availability at night (Rysgaard et al. 1999, Risgaard-Petersen et al. 2004). In a detailed study of the microbial communities associated with these sediments from July 2009 to May 2010, it was noted that the shallower sites at Jennycliff and Cawsand contained peaks in abundances of diatom and cyanobacterial species during summer months (K. Tait pers. comm.). Further measurements and analysis are required to fully understand the temporal changes and links between AOB *amoA* gene abundance and nitrification rates within these sediments.

Comparisons of the *amoA*-derived AOB community using PCR-DGGE also indicated sediment type to be a major factor in determining AOB community structure. However, depth was equally important: despite the lower AOB *amoA* gene abundance and ammonia oxidation at the muddier sites, there were no differences in the AOB *amoA* gene DGGE profiles between Jennycliff and Cawsand (Fig. 2A). In contrast, the DGGE profiles at Rame Mud and L4 did differ from each other and from those from Jennycliff and Cawsand (Fig. 2A). This difference in community composition with depth is more likely due to differences in factors such as light, nutrients, sedimentation, seasonal stratification and vertical mixing rather than depth per se. A small number of samples from Rame Mud and L4 were also analysed in detail using a functional gene microarray composed of AOB *amoA* archetype probes, indicating the presence of AOB previously found within marine sediments, with a smaller representation of AOB from estuarine communities, as would be expected in these predominantly marine sediment communities (Fig. 3A). Unlike the DGGE data, this indicated no differences in the AOB *amoA*-derived communities at L4 and Rame mud. However, the DGGE analysis picked up 56 unique bands at all sites: this is double

the number of AOB archetypes known to exist (Bouskill et al. 2011). It is likely that the DGGE is detecting fine-detail changes within the major clades identified by the microarray (Fig. 3A). Both DGGE and microarray analysis failed to detect seasonal changes to the AOB *amoA* community, indicating that the same community was present throughout the year. However, the DGGE analysis revealed a gradual shift in the AOB population through time for Jennycliff, Cawsand and Rame Mud sediments (Fig. 2). As the microarray data did not detect changes in community composition between July 2008 and March 2009, it is likely that these changes are also due to fine-detail changes within the major clades identified. Although no changes through time were detected within L4 sediments, the lack of this response may be due to the less complete dataset for this site. Alternatively, L4, the furthest from shore, and therefore furthest from the terrestrial or estuarine influence, may be less susceptible to disturbance of the established community from periodic fluctuations in salinity, allochthonous organic matter supply and seeding of the site with estuarine microbes.

Within this study, there was no correlation between AOA *amoA* gene abundance and nitrification rate. This is consistent with several other studies comparing AOA *amoA* gene abundance and activity in estuarine and coastal sediments (Magalhães et al. 2009, Wankel et al. 2011). Although abundance was higher at the deeper sites than the shallow sites, deciphering the temporal and spatial patterns in AOA abundance was made more difficult by the higher spatial variation amongst measurements (Fig. 1), and this likely obscured any temporal trends. Aside from the unusually high peaks in abundance at L4 in July and September of 2009 (Fig. 1H), like AOB *amoA* genes, AOA *amoA* gene abundance tended to be at its lowest in the summer months. In addition, the bimonthly sampling period may have also been too infrequent to pick up on rapid changes such as periodic pulses of organic matter or resuspension of sediment material. Other than salinity, one of the key factors thought to influence the relative distribution of AOA versus AOB is ammonium concentration: AOB tend to be associated with high substrate concentrations, whereas the AOA are considered to be oligotrophic (Coolen et al. 2007, Bouskill et al. 2012, Horak et al. 2013). Cultured representatives of the AOA have much higher affinities for ammonia when compared to the AOB (Martens-Habbena et al. 2009). Several AOA have also been shown to have low thresholds for ammonium and ammonia. Published data have shown the predominantly marine Crenarchaeota group I.1a to be inhibited by ammonium and ammonia concentrations in the range of 1 to 20 mM and 18 to 145 µM (Hatzenpichler 2012). This sensitivity of the group I.1a to ammonium concentrations may provide an advantage for AOB when ammonium levels are high. Calculations of porewater ammonium concentrations indicated levels fluctuated between a minimum of <1 µM and a maximum of 13 µM (at Cawsand in July 2010) and an average of 3.5 µM across all sites, concentrations that would be expected to, at the very most, only periodically inhibit some but not all AOA.

An alternative explanation for the lack of correlation between AOA *amoA* gene abundance, nitrification rates or any other environmental variable measured within this study could be the ATU used to inhibit ammonia oxidation. The study of Santoro & Casciotti (2011) suggested that archaeal *amoA* were not completely inhibited by ATU. They reported a 58% inhibition of nitrification at 0.09 mM, but 100% inhibition at 0.86 mM. As a result of this finding, the final concentration of ATU used in this study was 0.9 mM, similar to the concentration used by Santoro & Casciotti (2011) to completely inhibit nitrification. However, it may be possible that, even at this concentration, not all AOA in our study were completely inhibited.

Although the genome of *Nitrosopumilus maritimus* SCM1 implies a potential for mixotrophic growth (Walker et al. 2010), and reports of mixotrophic growth of Crenarchaeota group 1.1b, also referred to as the 'soil lineage' (Teira et al. 2006, Hatzenpichler et al. 2008, Mußman et al. 2011), has provided increasing evidence that terrestrial AOA may not be exclusively autotrophic, mixotrophic growth has not been demonstrated for marine lineages. Similarly, it is known the AOB ammonia monooxygenase enzyme has alternate substrates, such as methane and carbon monoxide (Ward 1990), but multi-functionality of the AOA ammonia monoxygenase had not yet been proven. The continued high abundance of AOA *amoA* genes at each site and throughout the 3 yr period study implies an important role for the AOA within the western English Channel sediments examined. The detection of the *amoA* gene does not necessarily signal that an organism is carrying out ammonia oxidation (Prosser & Nicol 2008, Stahl & de la Torre 2012). But it is possible that, in contrast to the AOB, the AOA in the sediments studied respond to changing substrate availability by a shift in activity rather than abundance. For example, in a study of ammonia-oxidising microbes in waters of Puget Sound, depth profiles of ammonia oxidation rates correlated with AOA *amoA* transcripts, but not AOA *amoA* gene copies (Horak et al. 2013).

The AOA *amoA* gene PCR-DGGE data indicated that there were no differences in community composition over time. There were also no differences in community composition at Jennycliff, Cawsand or Rame, but there were differences in community composition between Rame Mud and L4 (Fig. 2E). This was also evident in the microarray data (Fig. 3B). Differences in community composition were due to a consistently higher signal for archetypes AOA5, AOA20 and AOA27 in Rame than in L4 samples (Fig. 3B). AOA5 was derived from the Bahía del Tóbari, Mexico, a tropical saline estuary receiving substantial amounts of ammonium in agricultural runoff. Near identical sequences have also been found in estuarine sediments of the Zuari River, India (Singh et al. 2010) and the Pearl River estuary in China (Cao et al. 2013). AOA20 and AOA27 were based on sequences from corals and California beach sediments, respectively, but again have been found in sediments in the Pearl River estuary (Cao et al. 2013) and also sponges (Steger et al. 2008). A combination of differences including sediment particle size alongside factors associated with depth, as discussed above, may be driving the differences in community composition at L4. In contrast to the AOA PCR-DGGE data, the microarray data indicated a shift in community composition occurred between July 2008 and March 2009. However, the PCR-DGGE results are based on presence/absence data and, thus, cannot detect changes in relative abundance of specific AOA *amoA* clades, as seen in the microarray data.

CONCLUSIONS

This study has shown that although AOA *amoA* genes were more abundant within sediments in the western English Channel, measurements of AOB, and not AOA, *amoA* gene abundance correlated with benthic ammonia oxidation rates. AOB *amoA* gene abundance and ammonia oxidation measurements were highly correlated with sediment type, indicating a preference for sediments with larger particle size, possibly due to higher oxygen penetration into sandier sediments or higher concentrations of inhibitory sulphide within muddier sediments. Temporal changes to the abundance of AOB *amoA* genes and ammonia oxidation were also evident, with both decreasing during summer months, but further study is required to determine the cause of these decreases within the different sediments examined. The lack of correlation between AOA *amoA* abundance, ammonia oxidation rates or any of the environmental variables measured within this study was likely influenced by the higher spatial variation amongst measurements, which may have obscured temporal trends, and also the bimonthly sampling, which was likely too infrequent to capture temporal variability in organic matter deposition. Higher frequency measurements of transcript rather than gene abundance may provide a more accurate representation of the contribution of the AOB and AOA to rates of ammonia oxidation in sediments of the western English Channel.

Acknowledgements. The work forms part of the PML Benthic Survey and was funded in part by the NERC programme Oceans 2025, NERC National Capability and the US NSF Biocomplexity program. Thanks to the crew of 'Quest' for collecting the sample and Malcolm Woodward for overseeing the nutrient analysis.

LITERATURE CITED

Abell GC, Revill AT, Smith C, Bissett AP, Volkman JK, Robert SS (2010) Archaeal ammonia oxidizers and *nirS*-type denitrifiers dominate sediment nitrifying and denitrifying populations in a subtropical macrotidal estuary. ISME J 4:286–300

Alonso-Sáez L, Waller AS, Mende DR, Bakker K and others (2012) Role for urea in nitrification by polar marine Archaea. Proc Natl Acad Sci USA 109:17989–17994

Anderson M, Gorley RN, Clarke RK (2008) Permanova+ for Primer: guide to software and statistical methods. PRIMER-e, Plymouth

Beman JM, Roberts KJ, Wegley L, Rohwer F, Francis CA (2007) Distribution and diversity of archaeal ammonia monooxygenase genes associated with corals. Appl Environ Microbiol 73:5642–5647

Beman JM, Popp BN, Francis CA (2008) Molecular and biogeochemical evidence for ammonia oxidation by marine Crenarchaeota in the Gulf of California. ISME J 2: 429–441

Bernhard AE, Donn T, Giblin AE, Stahl DA (2005) Loss of diversity of ammonia-oxidizing bacteria correlates with increasing salinity in an estuary system. Environ Microbiol 7:1289–1297

Bernhard AE, Tucker J, Giblin AE, Stahl DA (2007) Functionally distinct communities of ammonia-oxidizing bacteria along an estuarine salinity gradient. Environ Microbiol 9:1439–1447

Bernhard AE, Landry ZC, Blevins A, de la Torre JR, Giblin AE, Stahl DA (2010) Abundance of ammonia-oxidizing archaea and bacteria along an estuarine salinity gradient in relation to potential nitrification rates. Appl Environ Microbiol 76:1285–1289

Biller SJ, Mosier AC, Wells GF, Francis CA (2012) Global biodiversity of aquatic ammonia-oxidizing archaea is partitioned by habitat. Front Microbiol 3:252

Bouskill NJ, Eveillard D, O'Mullan G, Jackson GA, Ward BB (2011) Seasonal and annual reoccurrence in beta-proteobacterial ammonia oxidizing bacterial population structure. Environ Microbiol 13:872–886

Bouskill NJ, Eveillard D, Chien D, Jayakumar A, Ward BB (2012) Environmental factors determining ammonia-oxidizing organism distribution and diversity in marine environments. Environ Microbiol 14:714–729

Bowen JL, Kearns PJ, Holcomb M, Ward BB (2013) Acidification alters the composition of ammonia-oxidizing microbial assemblages in marine mesocosms. Mar Ecol Prog Ser 492:1–8

Caffrey JM, Bano N, Kalanetra K, Hollibaugh JT (2007) Ammonia oxidation and ammonia-oxidizing bacteria and archaea from estuaries with differing histories of hypoxia. ISME J 1:660–662

Cao H, Auguet JC, Gu JD (2013) Global ecological pattern of ammonia-oxidizing archaea. PLoS ONE 8:e52853

Clarke KR, Ainsworth M (1993) A method of linking multivariate community structure to environmental variables. Mar Ecol Prog Ser 92:205–219

Clarke KR, Gorley RN (2006) PRIMER v6: user manual/tutorial. PRIMER-E, Plymouth

Coolen MJL, Abbas B, Van Bleijswijk J, Hopmans EC and others (2007) Putative ammonia-oxidizing Crenarchaeota in suboxic waters of the Black Sea: a basin-wide ecological study using 16S ribosomal and functional genes and membrane lipids. Environ Microbiol 9: 1001–1016

Eriksson PG, Svensson JM, Carrer GM (2003) Temporal changes and spatial variation of soil oxygen consumption, nitrification and denitrification rates in a tidal salt marsh of the Lagoon of Venice, Italy. Estuar Coast Shelf Sci 58:861–871

Francis CA, O'Mullan GD, Ward BB (2003) Diversity of ammonia monooxygenase (*amoA*) genes across environmental gradients in Chesapeake Bay sediments. Geobiology 1:129–140

Francis CA, Roberts KJ, Beman JM, Santoro AE, Oakley BB (2005) Ubiquity and diversity of ammonia-oxidising archaea in water columns and sediments of the ocean. Proc Natl Acad Sci USA 102:14683–14688

Grasshoff K (1983) Determination of nitrite. In: Grasshof K, Ehrhardt M, Kremling K (eds) Methods of seawater analysis, 2nd edn. Werlag Chemie, Weinheim, p 139–142

Hansen JI, Henriksen K, Blackburn TH (1981) Seasonal distribution of nitrifying bacteria and rates of nitrification in coastal marine sediments. Microb Ecol 7:297–304

Hatzenpichler R (2012) Diversity, physiology, and niche differentiation of ammonia-oxidizing archaea. Appl Environ Microbiol 78:7501–7510

Hatzenpichler R, Lebedeva EV, Spieck E, Stoecker K, Richter A, Daims H, Wagner M (2008) A moderately thermophilic ammonia-oxidizing crenarchaeote from a hot spring. Proc Natl Acad Sci USA 105:2134–2139

Horak REA, Qin W, Schauer AJ, Armbrust EV and others (2013) Ammonia oxidation kinetics and temperature sensitivity of a natural marine community dominated by Archaea. ISME J 7:2023–2033

Hornek R, Pommerening-Röser A, Koops HP, Farnleitner AH, Kreuzinger N, Kirschner A, Mach RL (2006) Primers containing universal bases reduce multiple *amoA* gene specific DGGE band patterns when analysing the diversity of beta-ammonia oxidizers in the environment. J Microbiol Methods 66:147–155

Jin T, Zhang T, Ye L, Lee OO, Wong YH, Qian PY (2011) Diversity and quantity of ammonia-oxidizing Archaea and Bacteria in sediment of the Pearl River estuary, China. Appl Microbiol Biotechnol 90:1137–1145

Joye SB, Hollibaugh JT (1995) Influence of sulfide inhibition of nitrification on nitrogen regeneration in sediments. Science 270:623–625

Kitidis V, Laverock B, McNeil CL, Beesley A and others (2011) Impact of ocean acidification on benthic and water column ammonia oxidation. Geophys Res Lett 38 L21603, doi:10.1029/2011GL049095

Lam P, Jensen MM, Lavik G, McGinnis DF and others (2007) Linking crenarchaeal and bacterial nitrification to anammox in the Black Sea. Proc Natl Acad Sci USA 104: 7104–7109

Laverock B, Smith CJ, Tait K, Osborn AM, Widdicombe S, Gilbert JA (2010) Bioturbating shrimp alter the structure and diversity of bacterial communities in coastal marine sediments. ISME J 4:1531–1544

Laverock B, Tait K, Gilbert JA, Osborn AM, Widdicombe S (2014) Impacts of bioturbation on the spatio-temporal distribution of bacterial and archaeal nitrogen-cycling genes in coastal sediments. Environ Microbiol Rep 6: 113–121

Leininger S, Urich T, Schloter M, Schwark L and others (2006) Archaea predominate among ammonia-oxidizing prokaryotes in soils. Nature 442:806–809

Li YH, Gregory S (1974) Diffusion of ions in sea water and in deep sea sediments. Geochim Cosmochim Acta 38: 703–714

Magalhães CM, Machado A, Bordalo AA (2009) Temporal variability in the abundance of ammonia-oxidizing bacteria vs. archaea in sandy sediments of the Douro River estuary, Portugal. Aquat Microb Ecol 56:13–23

Martens-Habbena W, Berube PM, Urakawa H, de la Torre JR, Stahl DA (2009) Ammonia oxidation kinetics determine niche separation of nitrifying Archaea and Bacteria. Nature 461:976–979

Mincer TJ, Church MJ, Taylor LT, Preston C, Karl DM, DeLong EF (2007) Quantitative distribution of presumptive archaeal and bacterial nitrifiers in Monterey Bay and the North Pacific Subtropical Gyre. Environ Microbiol 9: 1162–1175

Moin NS, Nelson KA, Bush A, Bernhard AE (2009) Distribution and diversity of archaeal and bacterial ammonia oxidizers in salt marsh sediments. Appl Environ Microbiol 75:7461–7468

Mosier AC, Francis CA (2008) Relative abundance and diversity of ammonia-oxidizing archaea and bacteria in the San Francisco Bay estuary. Environ Microbiol 10: 3002–3016

Mußmann M, Brito II, Pitcher A, Damsté JSS and others (2011) Thaumarchaeotes abundant in refinery nitrifying sludges express *amoA* but are not obligate autotrophic ammonia oxidizers. Proc Natl Acad Sci USA 108: 16771–16776

Norton JM, Klotz MG, Stein LY, Arp DJ and others (2008) Complete genome sequence of *Nitrosospira multiformis*, an ammonia-oxidizing bacterium from the soil environment. Appl Environ Microbiol 74:3559–3572

Prosser JI, Nicol GW (2008) Relative contributions of archaea and bacteria to aerobic ammonia oxidation in the environment. Environ Microbiol 10:2931–2941

Risgaard-Petersen N, Meyer RL, Schmid MC, Jetten MSM, Enrich-Prast A, Rysgaard S, Revsbech NP (2004) Anaerobic ammonium oxidation in an estuarine sediment. Aquat Microb Ecol 36:293–304

Rotthauwe JH, Witzel KP, Liesack W (1997) The ammonia monooxygenase structural gene *amoA* as a functional

marker: molecular fine-scale analysis of natural ammonia-oxidizing populations. Appl Environ Microbiol 63: 4704–4712

Rysgaard S, Thastum P, Dalsgaard T, Christensen PB, Sloth NP (1999) Effects of salinity on NH_4^+ adsorption capacity, nitrification, and denitrification in Danish estuarine sediments. Estuaries 22:21–30

Santoro AE, Casciotti KL (2011) Enrichment and characterization of ammonia-oxidizing archaea from the open ocean: phylogeny, physiology and stable isotope fractionation. ISME J 5:1796–1808

Santoro AE, Francis CA, de Sieyes NR, Boehm AB (2008) Shifts in the relative abundance of ammonia-oxidizing bacteria and archaea across physicochemical gradients in a subterranean estuary. Environ Microbiol 10:1068–1079

Seitzinger SP, Gardner WS, Spratt AK (1991) The effect of salinity on ammonium sorption in aquatic sediments: implications for benthic nutrient recycling. Estuaries 14: 167–174

Shen JP, Zhang LM, Zhu YG, Zhang JB, He JZ (2008) Abundance and composition of ammonia-oxidizing bacteria and ammonia-oxidizing archaea communities of an alkaline sandy loam. Environ Microbiol 10:1601–1611

Singh SK, Verma P, Ramaiah N, Chandrashekar AA, Shouche YS (2010) Phylogenetic diversity of archaeal 16S rRNA and ammonia monooxygenase genes from tropical estuarine sediments on the central west coast of India. Res Microbiol 161:177–186

Smyth TJ, Fishwick JR, Al-Moosawi L, Cummings DG and others (2010) A broad spatio-temporal view of the Western English Channel observatory. J Plankton Res 32: 585–601

Stahl DA, de la Torre JR (2012) Physiology and diversity of ammonia-oxidizing Archaea. Annu Rev Microbiol 66: 83–101

Steger D, Ettinger Epstein P, Whalan S, Hentschel U, De Nys R, Wagner M, Taylor MW (2008) Diversity and mode of transmission of ammonia-oxidizing archaea in marine sponges. Environ Microbiol 10:1087–1094

Sweerts JPRA, Kelly CA, Rudd JWM, Hesslein R, Cappenberg TE (1991) Similarity of whole-sediment molecular diffusion coefficients in freshwater sediments of low and high porosity. Limnol Oceanogr 36:335–342

Tait K, Laverock B, Widdicombe S (2014) Response of an arctic sediment nitrogen cycling community to increased CO_2. Estuaries Coasts 37:724–735

Taroncher-Oldenburg G, Griner EM, Francis CA, Ward BB (2003) Oligonucleotide microarray for the study of functional gene diversity in the nitrogen cycle in the environment. Appl Environ Microbiol 69:1159–1171

Teira E, Van Aken H, Veth C, Herndl GJ (2006) Archaeal uptake of enantiomeric amino acids in the meso- and bathypelagic waters of the North Atlantic. Limnol Oceanogr 51:60–69

Thompson SP, Paerl HW, Go MC (1995) Seasonal patterns of nitrification and denitrification in a natural and a restored salt marsh. Estuaries 18:399–408

Treusch AH, Leininger S, Kletzin A, Schuster SC, Klenk HP, Schleper C (2005) Novel genes for nitrite reductase and Amo related proteins indicate a role of uncultivated mesophiliccrenarchaeota in nitrogen cycling. Environ Microbiol 7:1985–1995

Venter JC, Remington K, Heidelberg JF, Halpern AL and others (2004) Environmental genome shotgun sequencing of the Sargasso Sea. Science 304:66–74

Walker CB, De La Torre JR, Klotz MG, Urakawa H and others (2010) *Nitrosopumilus maritimus* genome reveals unique mechanisms for nitrification and autotrophy in globally distributed marine crenarchaea. Proc Natl Acad Sci USA 107:8818–8823

Wankel SD, Mosier AC, Hansel CM, Paytan A, Francis CA (2011) Spatial variability in nitrification rates and ammonia-oxidizing microbial communities in the agriculturally impacted Elkhorn Slough estuary, California. Appl Environ Microbiol 77:269–280

Ward BB (1990) Kinetics of ammonia oxidation by a marine nitrifying bacterium — methane as a substrate-analogue. Microb Ecol 19:211–225

Ward BB, Bouskill NJ (2011) The utility of functional gene arrays for assessing community composition, relative abundance, and distribution of ammonia-oxidizing bacteria and archaea. In: Klotz MG, Stein LY (eds) Methods in enzymology: research on nitrification and related processes, Vol 496. Academic Press, Burlington, MA, p 373–396

Ward BB, Kilpatrick KA (1990) Relationship between substrate concentration and oxidation of ammonium and methane in a stratified water column. Cont Shelf Res 10: 1193–1208

Ward BB, Eveillard D, Kirshtein JD, Nelson JD, Voytek MA, Jackson GA (2007) Ammonia-oxidizing bacterial community composition in estuarine and oceanic environments assessed using a functional gene microarray. Environ Microbiol 9:2522–2538

Wuchter C, Abbas B, Coolen MJL, Herfort L and others (2006) Archaeal nitrification in the ocean. Proc Natl Acad Sci USA 103:12317–12322

Zheng Y, Hou L, Newell S, Liu M and others (2014) Community dynamics and activity of ammonia-oxidizing prokaryotes in intertidal sediments of the Yangtze Estuary. Appl Environ Microbiol 80:408–419

Editorial responsibility: Ronald Kiene, Mobile, Alabama, USA

Submitted: February 7, 2014; Accepted: June 29, 2014
Proofs received from author(s): September 12, 2014

Appendix. Table 1A. Pearson's rank correlation coefficients calculated for all sediment sites. Colours highlight the ρ-values which had a significance value of $p < 0.001$. Red is a negative correlation and blue is a positive correlation. SSSA: sediment specific surface area. S: salinity. TC, TOC and TIC are total carbon, total organic carbon and total inorganic carbon. TN, TON, TIN are total nitrogen, total organic nitrogen and total inorganic nitrogen, respectively. PW: porewater. All other nutrients are bottom water concentrations. NH_4^+ oxid.: NH_4^+ oxidation rate in sediments. Ammonia-oxidising bacteria (AOB) and ammonia-oxidising archaea (AOA) *amoA* are square root-transformed gene abundances g^{-1} sediment

	Depth (m)	SSSA	*T*(°C)	S	TC	TOC	TIC	TN	TON	TIN	C:N	NO_2^-	NO_3^-	NH_4^+	SiO_3^{2-}	PO_4^{3-}	PW NH_4^+	NH_4^+ oxid.	AOB *amoA*
SSSA	–0.054																		
T(°C)	0.012	–0.016																	
S	0.172	0.093	0.060																
TC	–0.248	0.711	–0.011	0.033															
TOC	–0.103	0.555	–0.058	0.045	0.699														
TIC	–0.268	0.329	0.095	–0.011	0.561	–0.162													
TN	–0.029	0.619	–0.139	0.094	0.704	0.722	0.093												
TON	–0.033	0.580	–0.071	0.068	0.636	0.640	0.169	0.930											
TIN	–0.093	0.456	–0.152	0.118	0.547	0.763	–0.104	0.746	0.572										
C:N	0.175	–0.555	0.109	–0.044	–0.495	–0.551	–0.027	–0.807	–0.731	–0.706									
NO_2^-	–0.073	0.067	0.166	0.082	–0.099	–0.082	–0.043	–0.016	0.024	–0.096	–0.086								
NO_3^-	–0.154	0.036	–0.487	0.073	–0.078	–0.009	–0.153	0.078	0.036	0.024	–0.069	0.501							
NH_4^+	0.025	0.058	0.246	0.069	–0.009	0.008	0.016	–0.076	–0.064	0.014	0.069	0.375	0.114						
SiO_3^{2-}	–0.134	0.073	–0.209	0.120	–0.118	–0.077	–0.124	0.015	–0.011	–0.043	–0.042	0.660	0.899	0.286					
PO_4^{3-}	0.043	0.051	–0.424	0.065	–0.050	0.055	–0.135	0.176	0.137	0.232	–0.166	0.195	0.571	0.016	0.521				
PW NH_4^+	–0.202	–0.281	0.061	0.068	–0.171	–0.195	0.010	–0.137	–0.150	–0.004	0.072	0.174	0.076	0.210	0.104	–0.002			
NH_4^+ oxid.	0.203	–0.273	–0.235	0.076	–0.268	–0.174	–0.160	–0.213	–0.170	–0.210	0.311	–0.235	0.007	–0.092	–0.004	0.126	–0.033		
AOB *amoA*	0.373	–0.679	–0.091	0.124	–0.575	–0.444	–0.297	–0.480	–0.483	–0.338	0.508	–0.197	–0.040	–0.081	–0.063	0.071	–0.020	0.522	
AOA *amoA*	0.310	0.048	–0.136	0.116	–0.041	–0.004	–0.100	0.067	–0.025	0.151	–0.111	–0.055	0.123	–0.072	0.165	0.075	0.016	0.007	0.232